Hindawi
Shock and Vibration
Volume 2022, Article ID 2905960, 15 pages
https://doi.org/10.1155/2022/2905960

Research Article

Seismic Damage Assessment of Steel Buildings considering Viscoelastic Dampers in Near-Field Earthquake

Mohammad Javad Bashir Pour

Faculty of Project Management and Construction, University of Tehran, Tehran, Iran

Correspondence should be addressed to Mohammad Javad Bashir Pour; javad.bashirpour@ut.ac.ir

Received 4 April 2022; Revised 29 April 2022; Accepted 6 May 2022; Published 15 July 2022

Academic Editor: S. Mahdi S. Kolbadi

In this study, three flexural steel frames of 4, 8, and 12 floors were investigated. The frames were designed based on the standard guidelines and then subjected to nonlinear dynamic analysis. Damage to structures with the concept of inelastic behavior and, consequently, hysteresis energy is very close. Therefore, it can be said that hysteresis energy at these levels can be a significant criterion for designing or controlling the structure. The high dependence of hysteresis energy on structural damage has caused this concept and new structural design methods to be considered by researchers and engineers. In this research, the first three steel frames of 4, 8, and 12-story with medium bending frame system with statically equivalent method. Then, all frames under the effect of seven near-field accelerometers and seven far-field accelerometers were analyzed nonlinearly and dynamically. The purpose of this study is to investigate the distribution of damage, energy, relative displacement, roof displacement, and base shear in the studied frames. In the following, the necessity of using the reinforcement method to reduce the relative displacement is described based on the regulations, then viscoelastic dampers are used to strengthen and reduce the damage in the frames under study. The results show that despite the uniform distribution of resistance at the height of the floors, the hysteresis and damage distribution diagrams do not follow this distribution and the concentration of energy and damage is observed in one or more floors. Therefore, in order to make the best use of the maximum system capacity, the design of structures based on strength alone does not seem logical and other parameters such as hysteresis energy, which play a major role in structural member damage, should be considered in the design process. Viscoelastic dampers have been used for retrofitting. The results show that this type of damper has a great role in absorbing energy and reducing damage to buildings. By calculating the damage of floors and the damage of the whole structure, it was seen that the level of damage under near-field earthquakes was greater than that in distant earthquakes and also in structures with a higher number of floors. The results show that as the height of the structure increases, the base shear values increase. As dampers are added to the structural layers, the base shear values are highly reduced so that, for 4, 8, and 12 floor frames under distant field earthquakes, 54%, 45%, and 48% decrease, respectively, and near-field earthquakes decrease, by 55%, 68%, and 64%, respectively. Also, the effect of using viscoelastic dampers on reducing the damage of high-altitude frames has been more and shows good performance in reducing the damage under earthquakes in the near area.

1. Introduction

It is now well recognized that structures designed in line with existing regulations will be highly damaged by severe earthquakes [1]. Nevertheless, some seismic design criteria (especially in the initial design of structures) are still founded on elastic analysis and the application of a static force equivalent to an earthquake [2]. The forces applied by an earthquake rely on the elastic and plastic characteristics of the structure [3]. New building guidelines were developed by various organizations to meet these needs. Two related guidelines were VISION 2000 [4] published by the California Society of Structural Engineers (SEAOC), and the seismic renovation of buildings (BSSC), released by the federal emergency management agency (FEMA). Earthquake is a phenomenon causing a lot of energy to be released in the Earth in a short time [5]. The released energy inflicts strong vibrations in the upper areas of the Earth [6]. It

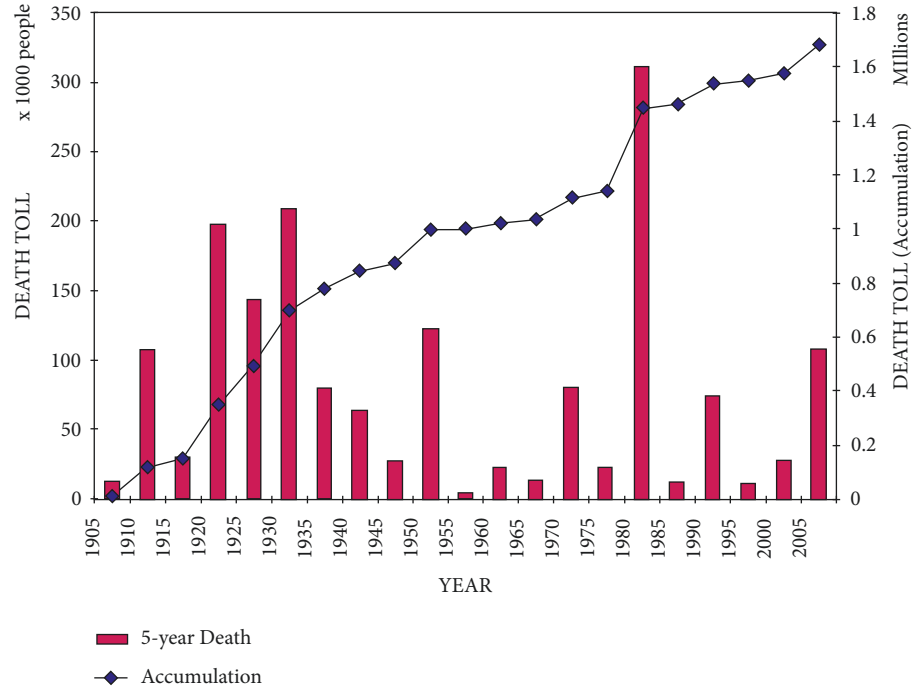

Figure 1: Loss of life caused by major earthquakes [4].

should be mentioned, however, that the closer the period of the building to the period of the earthquake, the higher the effects of the earthquake on the building structure (intensification phenomenon) [7]. Viscoelastic materials were first used to withstand earthquakes, dating back to 1993 in the United States, when seismic reinforcement was used in a 14-story Santa Clara country steel structure. Established in 1976, the structure was reinforced by 16 viscoelastic dampers [8].

In 1991, Zhang et al. installed three types of viscoelastic dampers with different specifications in a five-story steel building and used seismic table experiments, they investigated the factors affecting the efficiency of viscoelastic dampers, such as temperature, frequency, etc. They found that these types of dampers were found to have a great effect on reducing structural responses at all levels [9]. In 2002, Lee and Kim analyzed various methods for analyzing structures with viscoelastic dampers, such as direct integration, the principle of modulation overlap, and the modal strain energy method on 10- and 20-story structures, and compared the results [10]. In 2003, Tezkan and Uluka [11] subjected a 7-story steel frame and 10- and 20-story reinforced concrete frames to nonlinear dynamic analysis, and by examining the base shear, roof displacement, and absolute roof acceleration, they suggested that the presence of viscoelastic dampers in structures greatly reduced the structural responses because of the damping provided for them [11]. In 2004, Maine and Kim carried out a seismic test of a 5-story steel frame by a viscoelastic damper. Investigating viscoelastic dampers in the form of Chevron in different classes and under two temperatures of 24 and 30°C, they examined the efficiency of dampers and found that the acceleration responses had been greatly reduced by installing dampers in the structure. This decrease was greater at 24°C than at 30°C [12]. In 2000, Zimmer [13] examined the vulnerabilities and methods for improving steel structures using a variety of dampers, including viscous and viscoelastic dampers. For this end, a 9-story steel building was subjected to nonlinear dynamic analysis of seven accelerometers [14]. The results suggested that using the above dampers in the structure reduced displacement and failure in the structure and many columns remain in the elastic state [13].

2. Materials and Methods

2.1. Relative Energy Equation. Seismic loads are initially contractual in nature, and the seismic design forces designed by the regulations are generally much smaller than the forces applied to the structure during an earthquake (Figure 1). The energy incoming to the structure depends on both seismic characteristics such as frequency, intensity, and periodicity of strong motions and structural characteristics such as ductility, damping, periodicity, and hysteresis behavior [15]. In determining the input energy to structures, it is generally assumed that the periodicity of the structure is about the dominant periodicity of the earth. Because in this range, energy is independent of the dynamic properties of the structure [16].

This range is the constant velocity area as provided by to Newmark-Hall definitions [17]. Considering that the energy is proportional to the square of velocity, the incoming energy in this area will be stable [18]. However, this is not the case at higher and lower cycles (areas corresponding to constant displacement and constant acceleration) [19]. Based on equation (1) it integrate that equation regarding

to the variable u, it is seen that the second and third parts on equation (2) do not change from the state and can be expressed as equation (2). This value is equal to the relative kinetic energy (E_K') obtained using relative velocity as equation (3). The sentence to the right of equation (4) is conventionally known as the relative input energy (E_I').

$$\int m\ddot{u}\mathrm{d}u + \int c\dot{u}\mathrm{d}u + \int f_s\mathrm{d}u = -\int m\ddot{u}_g\,\mathrm{d}u, \tag{1}$$

$$\int m\ddot{u}\mathrm{d}u = \int\left(m\frac{\mathrm{d}\dot{u}}{\mathrm{d}t}\right)\mathrm{d}u = \frac{m\dot{u}^2}{2}, \tag{2}$$

$$E_K{}' = \frac{M\dot{u}^2}{2}, \tag{3}$$

$$E_I' = \int m\ddot{u}_g\,\mathrm{d}u. \tag{4}$$

The physical meaning of which is what occurs by the lateral force of the static average $-m\ddot{u}_g$ in displacement on a system equivalent to a fixed support, where the effect of rigid structural displacement is ignored. In other words, one can say if the structure of magnitude du displaces because of the effective force $P_{\text{eff}} = -m\ddot{u}_g$, the energy applied to the structure will be equal to $\mathrm{d}'E_i = m\ddot{u}_g\mathrm{d}u$ and it is integral, which is equation (4). Hence, the relative energy equation can be expressed as equation (5). According to equations (3) and (4), the levels of damping and absorbed energy do not change in the relative state compared to the absolute state as equation (6).

$$E_I' = E_K' + E_D + E_A = E_K' + E_D + E_S + E_H, \tag{5}$$

$$E_I - E_K = E_I' - E_K', \tag{6}$$

2.2. Cumulative Damage Indicators. Meeting cumulative damage from dynamic loading is one of the topics of interest for engineers [20]. This procedure is usually carried out by low-cycle fatigue relations or by calculating the energy absorbed by the system when loading time. In both cases, inelastic behavior is supposed for the systems before any damage is taken into account [21]. Attempts are made to use the former deformation indices in cumulative damage by extending the concept of ductility to cyclic loading. Bannon and Wenziano [22] introduced a normalized cumulative deformation damage index, which is the ratio of the total plastic deformation of the maximum of all half-cycles to yield deformation. The low-cycle damage model makes use of cumulative plastic deformation to represent damage. One of the first indices of this class was presented by Lemura [23]; which is a function of the sum of the nonlinear nonelastic deformation function of each half-cycle of response. Yao and Unze [24] provided a similar index based on rotational ductility conditions. This index indicated the damage to the member. However, the fixed values used in their formula depended on the characteristics of the member, so this index is not generally applicable [25].

2.3. Viscoelastic Dampers. The energy incoming to the structure can be divided into four parts in a nonlinear state: kinetic energy, damping energy, strain energy (potential), and yield energy (hysterical) [26]. Hardness (kd) and damping (cd) can be attributed to a viscoelastic damper at a given temperature and frequency. Assuming a small mass (md) for this damper, equation (7) of this system can be expressed similar to the normal degree of freedom system as a result of the sine load at a certain temperature and frequency [27]. In this case, the permanent displacement of this system will be sinusoidal. If the strain is applied, which is the ratio of the displacement of the damper to the thickness of the viscoelastic layer, one would say that the strain of this system will be sinusoidal [28] as equation (8), where γ_0, Δ, and h are the strain amplitude, displacement, and viscoelastic layer thickness, respectively. The force generated in this system is because of hardness and damping [29].

$$\gamma(t) = \gamma_0.\sin(\omega t), \tag{7}$$

$$\gamma = \frac{\Delta}{h}. \tag{8}$$

The part related to the hardness is the product of the damping hardness in the displacement and the one related to the damping is the product of the velocity multiplied by the damping of the damper [30]. Therefore, one would suggest that the force generated in this system will be in a form of a sinusoidal expression with phase difference relative to displacement [31]. Similarly, instead of force, the stress obtained by dividing the shear force on the surface of the viscoelastic material (A) is used (equation (9)), where τ_0 is the maximum shear stress and δ is the phase difference angle between stress and strain [32]. Using the viscoelastic linear law, the amplitude of stress and strain can be assumed to be proportional. In this case, equation (10) can be extended as equation (11).

$$\tau(t) = \tau_0\sin(\omega t + \delta), \tag{9}$$

$$\begin{aligned}\tau(t) = \gamma_0 G^*\sin(\omega t + \delta) = \gamma_0\big(&G^*\cos\delta\sin\omega t \\ &+ G^*\sin\delta\cos\omega t\big),\end{aligned} \tag{10}$$

$$\tau(t) = \gamma_0\left(G'\sin\omega t + G''\cos\omega t\right), \tag{11}$$

$$G^* = \left[G'^2 + G''^2\right]^{1/2}. \tag{12}$$

G^* is the combined shear modulus, G' shear storage modulus, and G'' shear loss modulus. By equating this expression in terms of force and by multiplying the hardness of the damper by the displacement and by multiplying the damping by the velocity, an expression for the hardness and damping of this damper is obtained (equation (12)). Using equations (13) and (14) by removing time from these equations, the stress-strain relationship can be determined by equation (15) that is shown in Figure 2.

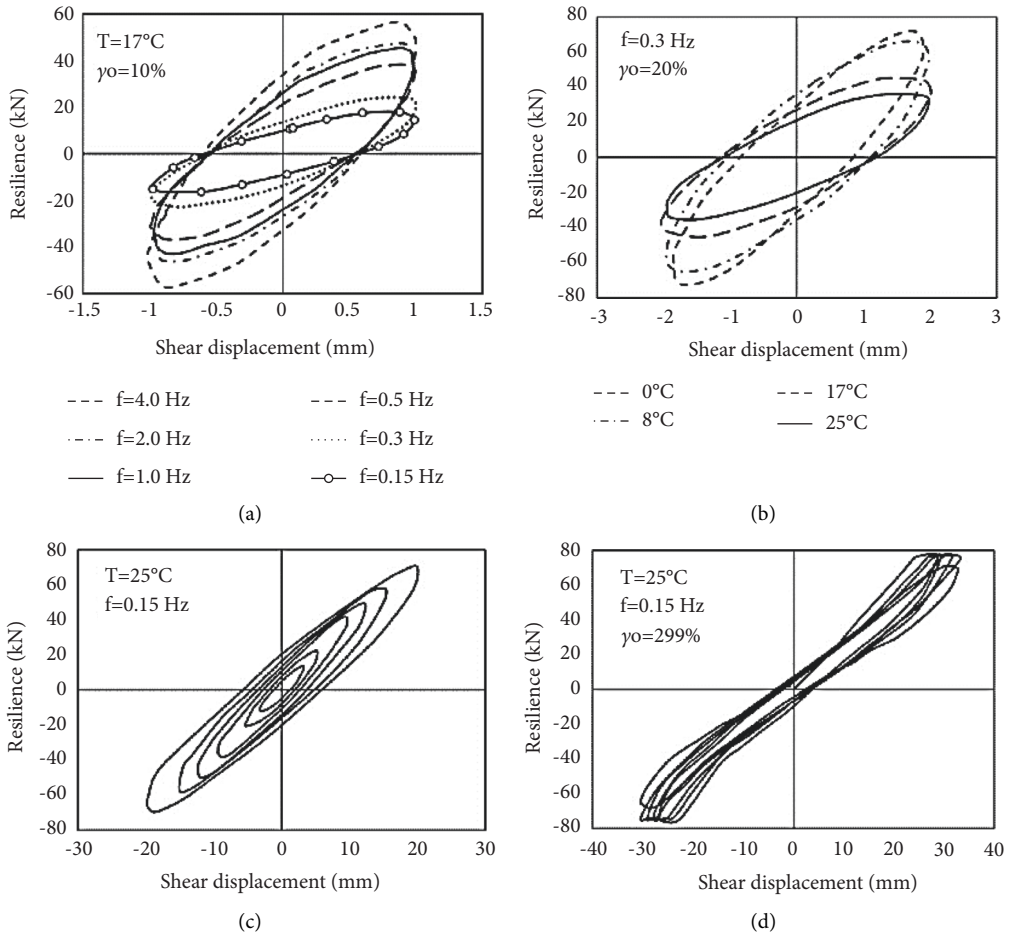

Figure 2: Viscoelastic damping residual curve [33]: (a) different excitation frequency; (b) different ambient temperature; (c) different shear strain amplitude; (d) damper failure.

$$K_d = \frac{G'.A}{h}, \tag{13}$$

$$C_d = \frac{G''.A}{\omega.h}, \tag{14}$$

$$\tau(t) = G'\gamma(t) \pm G''\sqrt{\gamma_0^2 - \gamma a(t)^2}. \tag{15}$$

The dissipation coefficient can be applied to evaluate the waste curve. The small size of this coefficient indicates the thinness of the dissipation curve and the low energy absorption capacity, and conversely, the larger the coefficient indicates the high energy absorption capacity [34]. The dissipation coefficient is defined as equation (16). High-frequency or low-temperature polymers are usually placed in glass areas, in which the dissipation coefficient is small and the material exhibits elastic behavior in this area, while this coefficient is greater in the transmutation region, so energy dissipation is assumed to be greater in this area [35]. The absorbed energy in each period is calculated per unit volume of viscoelastic matter as equation (13). The elastic energy stored in each period is also calculated as equation (17), where Δ_0 is the maximum displacement of the damper. Using the energies calculated in equations (18), the equivalent damping ratio can be estimated as equation (19).

$$\eta = \tan\delta = \frac{G''}{G'}, \tag{16}$$

$$E_d = \int_0^{T-\frac{\eta\pi}{\omega}} \tau\left(\frac{d\gamma}{dt}\right)dt = \pi\gamma_0^2 G'', \tag{17}$$

$$Es = K_d\Delta_0^2. \tag{18}$$

$$\xi = \frac{1}{4\pi}\frac{E_d}{E_s} = \frac{G''}{2G'}. \tag{19}$$

To specify the characteristics of the viscoelastic material, according to the results of the experiments, the ambient temperature can be used as the design base temperature, in addition to the increase in temperature due to energy absorption in the viscoelastic material [36].

2.4. Modeling of Structures with Viscoelastic Dampers. The results of the experiments suggest that the effects of higher modes are reduced and negligible using viscoelastic dampers in the building [37]. Accordingly, the results from the

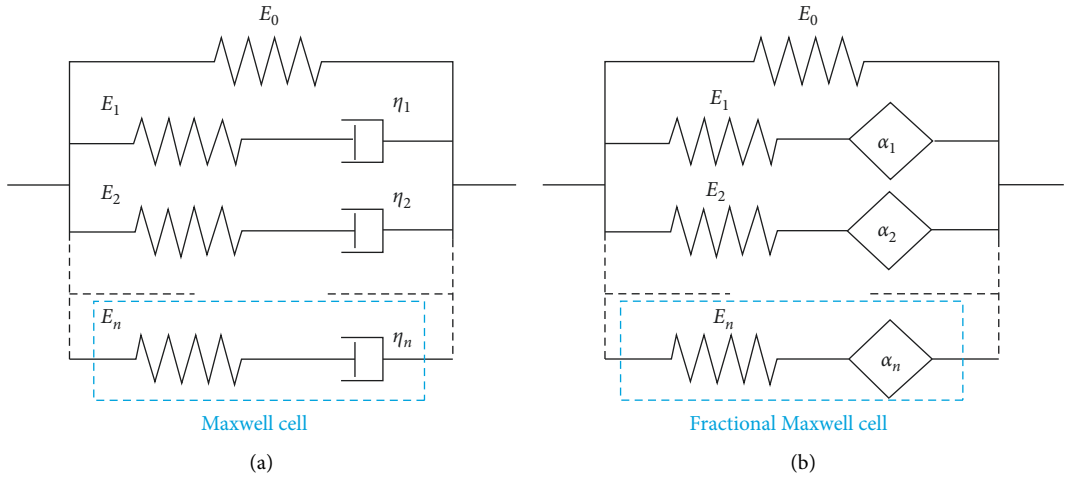

Figure 3: (a) Analytical and (b) fractal Maxwell model for viscoelastic materials [42].

analyses performed based on the first mode had a good coordination with the laboratory results, which is one of the strengths of the damper that makes the calculations simple and easy [38]. The behavior of viscoelastic materials is expressed as a combination of elastic and viscous behaviors. For linear elastic materials, the normal stress describe as equation (20), where E is the modulus of elasticity or the Young's modulus and ε is the axial strain [39]. For such cases, stress and strain are time-independent. This behavior can be modeled by a simple spring. For linear viscous, the resisting force is proportional to the velocity of motion [40]. The stress-strain relationship for a bar with cross section A and length L is stated as equation (21). So that c is the proportionality constant or the damping constant. In this case, strain and stress are time-dependent. Several mathematical models were proposed to describe the dynamic behavior of the viscoelastic case [41].

$$\sigma = E\varepsilon, \tag{20}$$

$$\sigma A = C\dot{U}. \tag{21}$$

In this model, the case is modeled as a linear spring and damper in series, so that the stresses in the dampers and springs are made equal and the total strain is made equal to the sum of the strain of each. This model is generally used in modeling liquid viscoelastic materials (equations (22) and (23)) so that σ_1 and ε_1 linear stresses and strains of the spring and σ_2 and ε_2 linear stresses and strains of the dampers (Figure 3)

$$\varepsilon = \varepsilon_1 + \varepsilon_2, \tag{22}$$

$$\sigma = \sigma_1 = \sigma_2. \tag{23}$$

2.5. Frames Studied in This Study. To assess the vulnerability of steel frames based on energy concepts, to compare the damage rate of floors and frames, as well as to provide a solution to reduce the damage rate in steel frame members, the medium flexural frame system was modeled as follows. Then, the lateral loading of each of the mentioned frames was performed under similar conditions and in line with the criteria stated in the building design regulations against earthquakes in a statically equivalent way [8]. The 4, 8, and 12-story frames were designed by the allowable stress method, relying on the equal resistance distribution in the floors. They were then exposed to seven scale-accelerated earthquake accelerations [43]. It was seen that the relative lateral displacement values of the floors in the frames under study were not within the permissible limits as set by the regulations, and the above frames needed to be reinforced. In this research, viscoelastic dampers were applied for retrofitting. Finally, after controlling the displacement according to the regulations, the level of damage in the above frames was compared before and after retrofitting and parameters such as roof displacement [44]. The base shear and values of hysteresis energy, residual energy, and the ratio of hysteresis energy to input energy were also investigated and compared.

Also, for reinforcement, a viscoelastic damper was added to the initial flexural frame in the middle openings of the frame in all classes. Nonlinear analysis of the time history of structures was performed using Perform 3D software [45]. The buildings in question were analyzed as time history under the effect of seven far-field earthquake accelerometers and seven near-field earthquake accelerometers, the characteristics of which are provided in the next section. The damping of all structures was 5% and selected according to the mass and hardness. In this research, the values contained in the seismic improvement instruction [46] were applied to obtain force-displacement diagrams of structural members. Two-line behavior was used to introduce the plastic joint in the columns. To perform nonlinear dynamic analysis of time history, it was necessary to select earthquake records. Thus, seven near-field earthquake records were selected, and these earthquakes turned into design earthquakes and then applied to frames [47]. Relatively complete specifications of these records were provided in near range earthquakes in Table 1, respectively, [47]. For better comparison, attempts

Table 1: Details of near-field earthquake records used in this research (this table is reproduced from) [47].

Earthquake	Component	Magnitude	PGA (g)	Distance from fault (km)	Year
Landers	JOS000	$M_S = 7.4$	0.274	21.2	1992/06/28
Kocaeli	ARC000	$M_S = 7.8$	0.218	17	1992/08/17
Imperial valley	H/VCT075	$M_S = 6.9$	0.122	43.5	1979/10/15
Tabas	BAJ/$L1$	$M_S = 7.4$	0.094	121.2	1978/09/16
Loma prieta	A3E090	$M_S = 7.1$	0.084	57	1989/10/18
Park field	C12320	$M_S = 6.1$	0.063	17.3	1969/06/28
San fernando	WTW025	$M_S = 6.6$	0.061	60.7	1971/02/09

were made to select far and near-field records from an earthquake so that other characteristics, such as frequency content, earthquake duration, and earthquake source conditions, are very close to each other.

2.6. Verification of Viscoelastic Damper Modeling. In order to confirm the accuracy of viscoelastic damper modeling in Perform 3D software, the 3-tier structure previously tested by Chang et al. [46] was modeled using the Kelvin mathematical model method in this software. As shown in Figure 4, the viscoelastic damper was placed diagonally across all floors and the specifications of the sections used in this structure are given in Table 2.

The viscoelastic damper placed in this structure was designed and evaluated under temperature of 28°C, frequency of 1.6 Hz, strain of 60% in lateral displacement of 0.5%, and damping of 15%. Also, the material of viscoelastic material applied in this experiment is 3M ISD 110 with shear storage modulus $G' = 0.06\,\text{KN/cm}^2$ and $\eta = 1$. Also, the hardness of the damper was equal to 3.5 KN/cm. The above structure was subjected to 0.5 g centrifugal earthquake. One of the clear features of viscoelastic dampers was the hysteresis curve of this type of damper, which is a combination of the curves of the viscous section, which is horizontally oval, and the elastic section, which is linear. Finally, the hysteresis curve of the viscoelastic damper was elliptical. In this section, the hysteresis curve of this damper was examined to validate the modeling of viscoelastic dampers in Perform 3D software. The following hysteresis curve was obtained from the Zhang experiment on the above structure under the centro earthquake.

Examining the hysteresis curves related to the experiment and the hysteresis curve resulting from modeling. It is seen that the hysteresis curve obtained from the modeling and the curve from the experiment were very similar and the time interval and the load was very close (Figure 5). Therefore, the accuracy of viscoelastic damper modeling was confirmed by Perform 3D software.

3. Results and Discussion

3.1. Investigation of Time History Results of the Input Energy of the Landers' Earthquake. The incoming energy of the structure under each earthquake is partly wasted because of damping and nonlinear behavior (hysteresis energy) and the rest is absorbed in the structure in a kinetic energies and elastic strain form, which is finally absorbed by the dampers after the earthquake. For instance, in Figures 6–8, the results

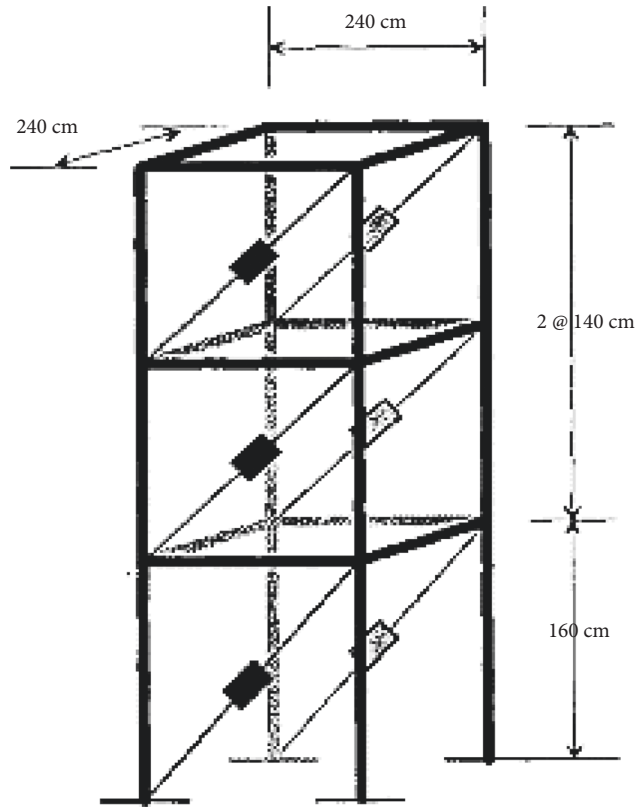

Figure 4: Dimensions and size of the building under test [46].

from analyzing the input energy are provided in different terms, under the Landers and Tabas records before and after the damping is added to the structure, in near-field earthquakes for all frame. Because descriptions of time history forms related to other earthquakes are duplicated, all cases were omitted. Figure 6 demonstrate the time history of the input energy of the 4-story frame under the Landers earthquake before and after the viscoelastic damper is added to the frame. From these diagrams, which are taken from Perform 3D software, one can see the effect of adding damper on reducing hysteresis energy and thus reducing the damage to the structure.

As seen in Figure 6, the red color in the diagram indicates the share of hysteresis energy entering the frame due to the near-field earthquake, which it is almost zero in Figure 6 and instead, a large portion of the input energy was absorbed by the viscoelastic damper, which shown in purple in the diagram, indicating the good efficiency of the viscoelastic damper on reducing the hysteresis energy on the frame,

Table 2: Specifications of the sections of the elements used [46].

Parameter	Beam			Column		
	First floor	Second floor	Third floor	First floor	Second floor	Third floor
Area (cm^2)	7	6.85	6.1	9.1	7.6	7.6
Moment of inertia (cm^4)	135	122	64.9	107	86	86
Bending anchor (cm^3)	28.5	29.6	18.9	29.9	24.3	24.3

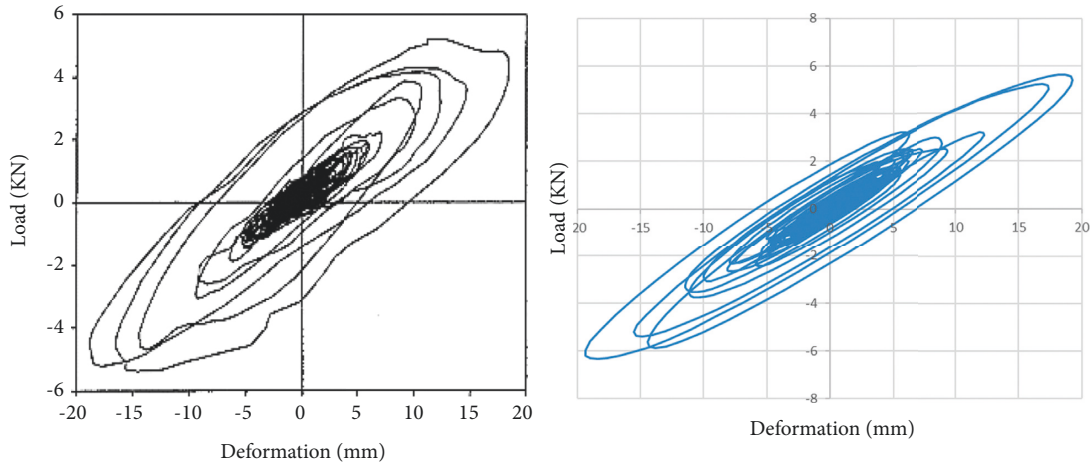

Figure 5: Curve of viscoelastic damping hysteresis under centrifugal earthquake, this figure is reproduced from reference [47], in comparison with extracted results from Perform3D.

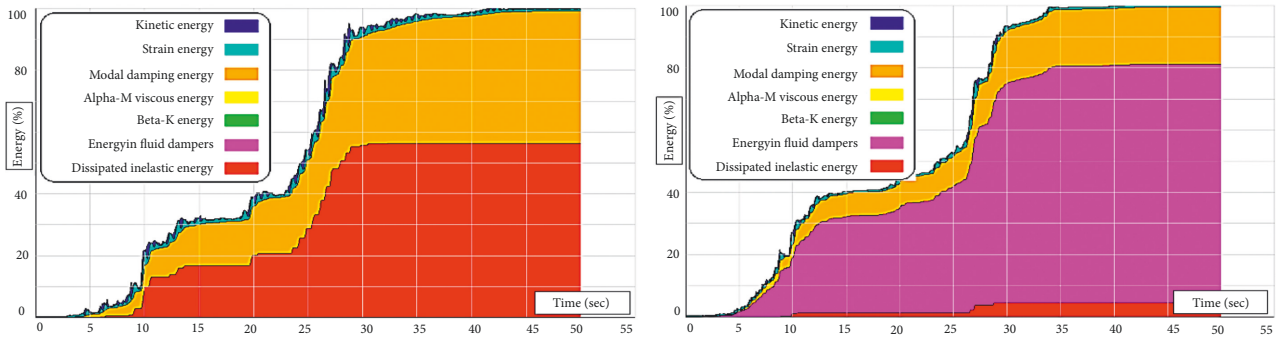

Figure 6: 4-story frame under record near Landers without and with dampers.

which directly pertaining to the damage. Also, looking at Figure 6, one may understand the difference in the level of hysteresis energy absorption with the entry of the structure into the nonlinear stage, under near-fault records. This difference being due to the existence of maximum acceleration, maximum speed, and maximum displacement in near-fault records as compared to near-fault records.

The results from the time history of the input energy of the 8-story frame under the earthquake near Landers before and after the viscoelastic is added damper to the frame are provided in Figure 7. Similar to the 4-story framework, one can understand that hysteresis energy contributes less than the total input energy to near-fault records. Also, as dampers are added to the frame, a large share of energy is absorbed by the dampers and the level of hysteresis energy absorbed by the members is directly reduced, which is directly related to structural damage. In this frame, hysteresis energy contribution has increased.

In this section, the results from the time history of the input energy of the 12-story frame under the Landers area earthquake before and after the viscoelastic damper is added to the frame are provided in Figures 8. The explanations of this section are similar to the explanations provided for the 8-story frame, and it is seen that as height of the structure increases, the share of hysteresis energy in the input energy rises.

3.2. Investigation of Hysteresis Energy in Structures. Hysteresis energy or plastic energy absorbed and dissipated in a structure is a function of time. The level of this energy in a structure is an indicator of the level of damage to the structure or its ductility, but cannot suggest the type of mechanism of yield and collapse. After seven acceleration maps of the field are applied near the frames and while performing nonlinear dynamic analysis, the level of hysteresis energy related to each

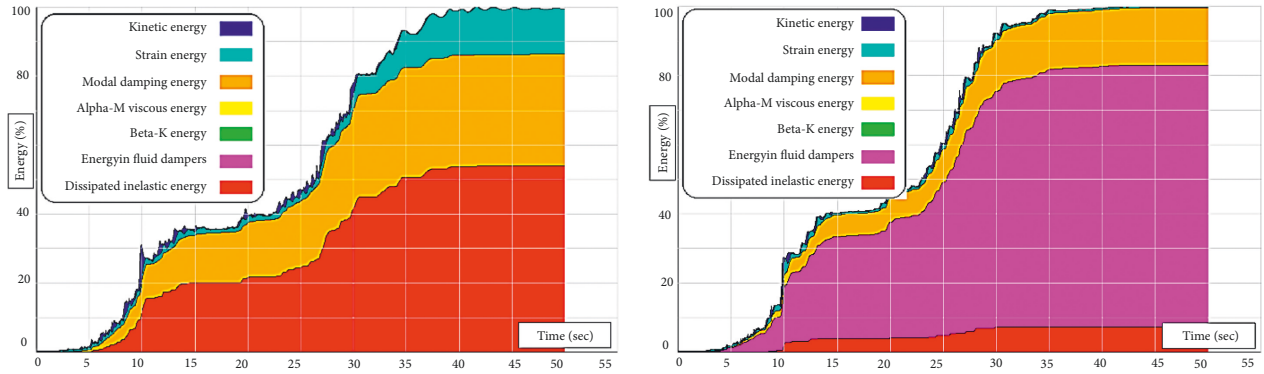

Figure 7: 8-story frame under record near Landers without and with dampers.

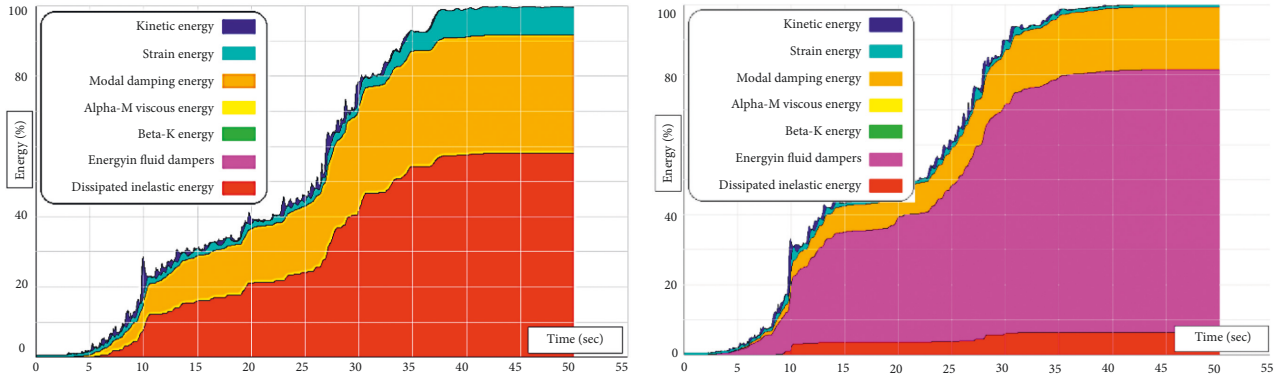

Figure 8: 12-story frame under record near Landers without and with dampers.

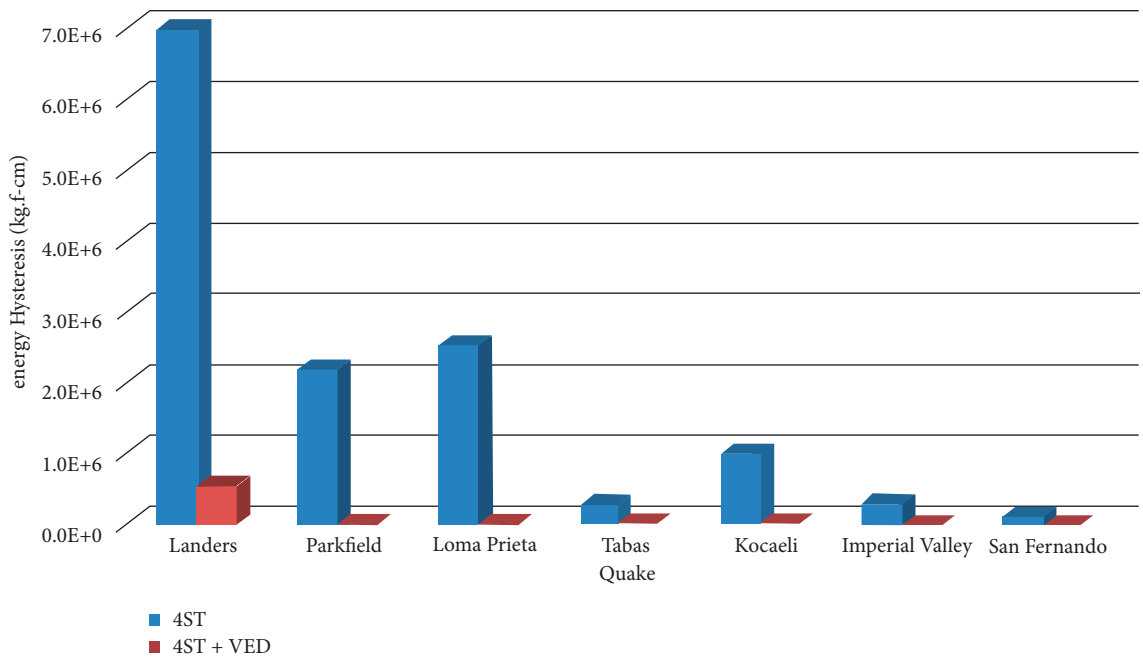

Figure 9: Hysteresis energy applied to a 4-story frame under near-field records in two modes, with and without dampers.

earthquake was calculated. In Figures 9 and 10, the results from the hysteresis energy of all frames were shown separately for the records before and after the damper is added to the classes. As seen from the diagrams, adding a damper to the structure reduces the level of hysteresis energy. The results from the hysteresis energy applied to the 4-story frame, under the far and near-field earthquakes with and without dampers, are presented in Figure 9.

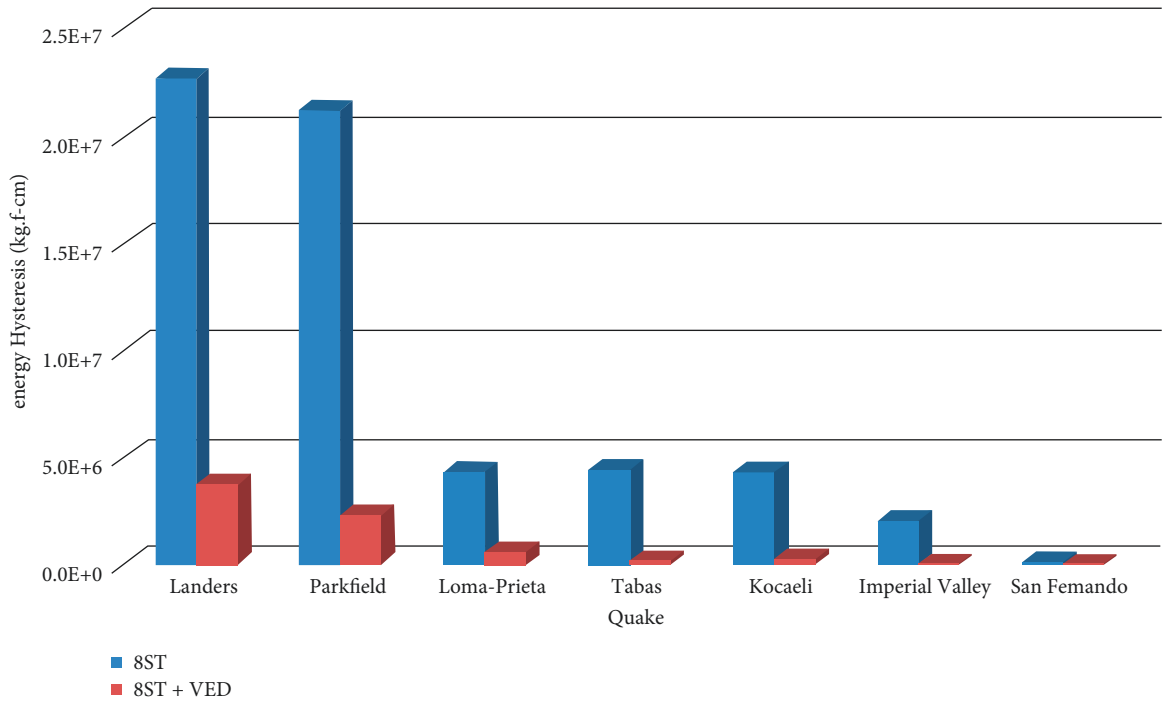

Figure 10: Hysteresis energy applied to the 8 8 floor frame under near-field records, in both modes with and without dampers.

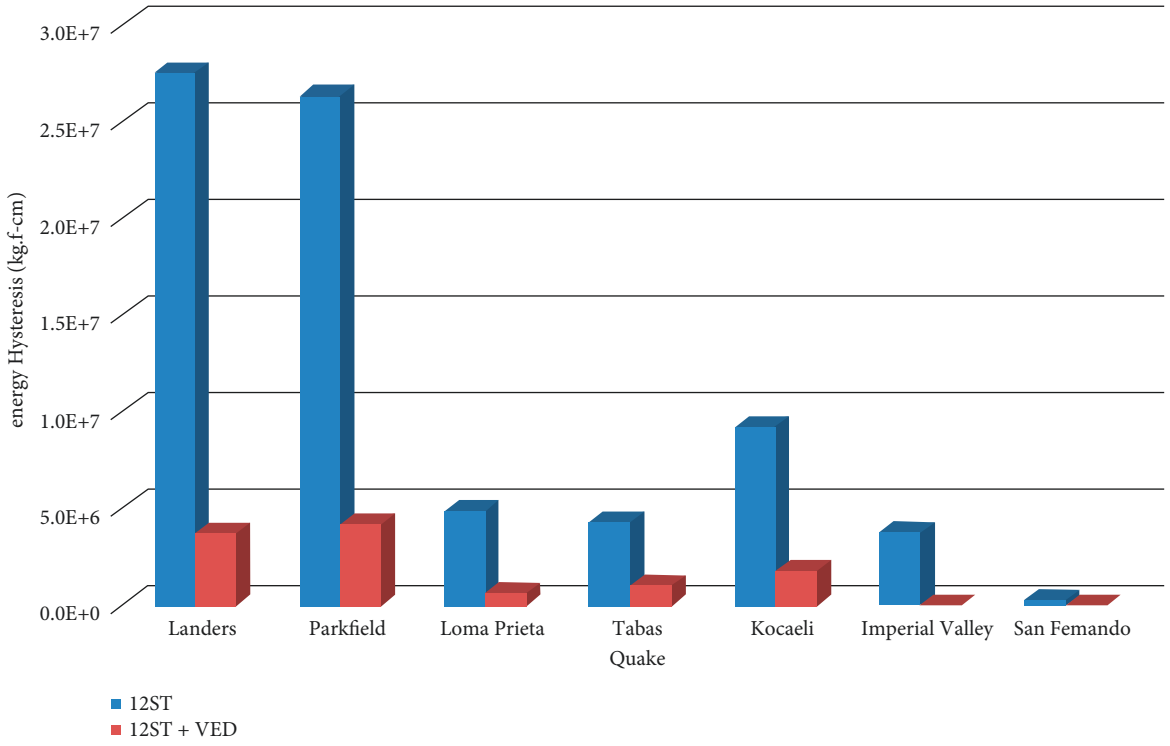

Figure 11: Hysteresis energy applied to the 12-floor frame under near-field records, in two modes with and without dampers.

The results related to the hysteresis energy applied to the 8-story frame under near-field earthquakes with and without dampers are shown in Figure 10.

The hysteresis energy results on the 12-story frame under near-field earthquakes with and without dampers are shown in Figure 11.

3.3. Investigation of Residual Energy in the Structure. In order to examine the effect of using viscoelastic dampers on reducing the hysteresis energy applied to structural members and the amount of damage caused in them, an index called residual energy was calculated in the frames under study. Residual energy in frames refers to the

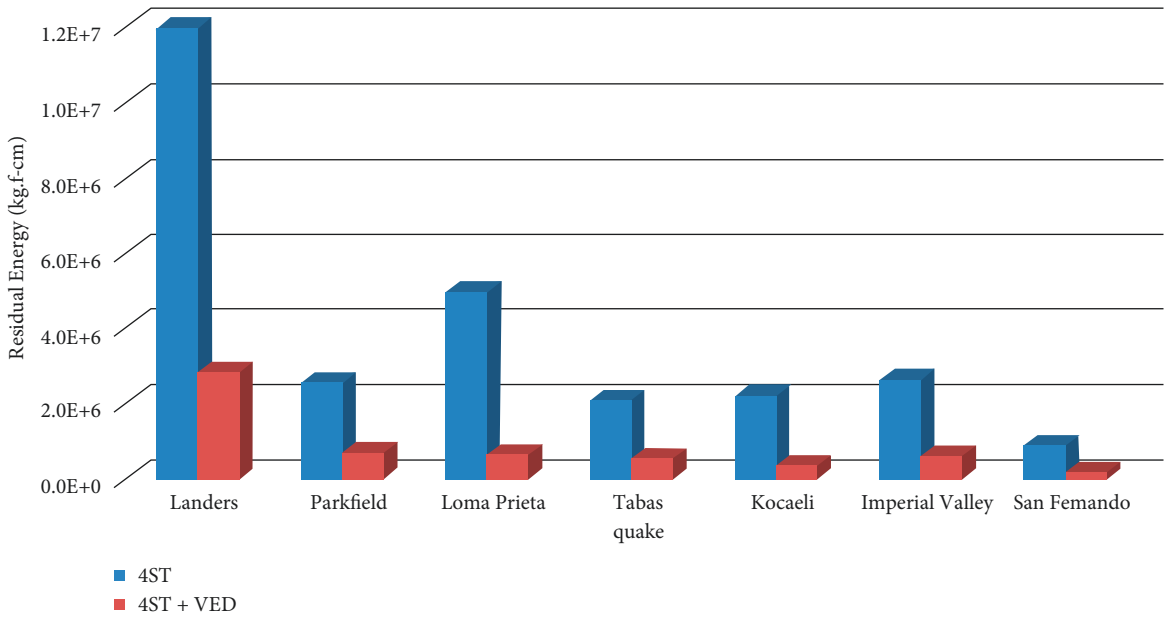

Figure 12: Residual energy diagram in a 4-story frame under near-field records, in two modes with and without dampers.

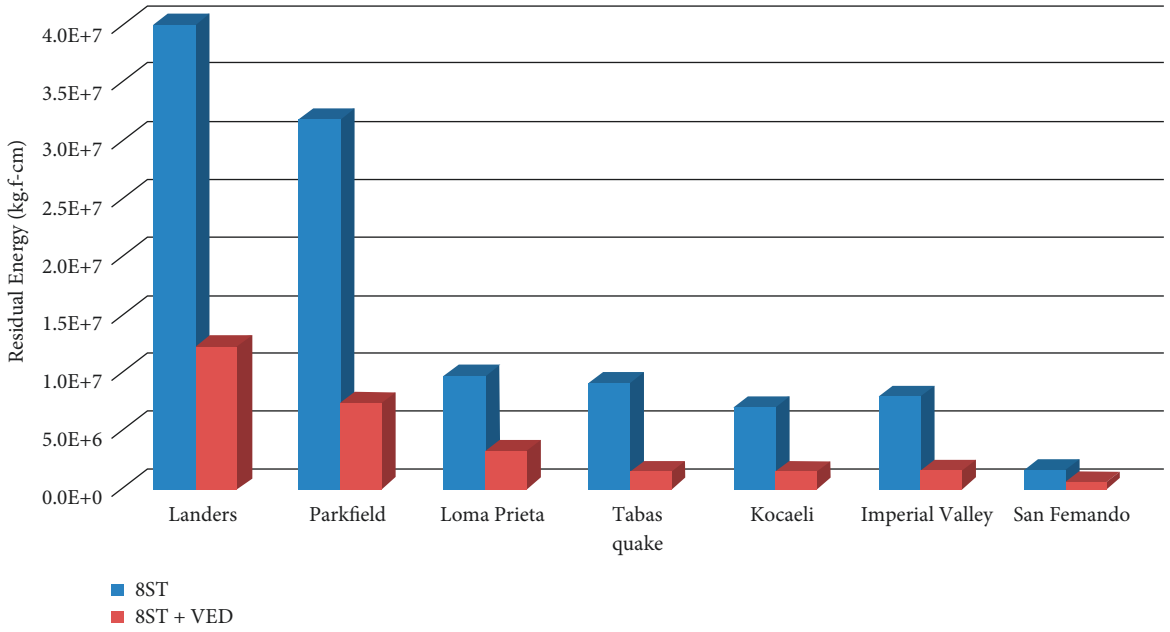

Figure 13: Residual energy diagram in an 8-story frame under near-field records, in two modes with and without dampers.

difference of energy absorbed by viscoelastic dampers from the energy incoming to the structure as it shows the effect of using dampers on reducing the hysteresis energy incoming to the structures. Residual energy diagrams for frames of 4, 8, and 12 floors under near-field earthquakes are illustrated in Figures 12–14, respectively. The results related to residual energy in a 4-story frame under near-field earthquakes with and without dampers are provided in Figure 12.

The results for residual energy in the 8-story frame under near-field earthquakes with and without dampers are shown in Figure 13.

The results related to the residual energy in the 12-story frame, under near-field earthquakes with and without dampers, are shown in Figure 14.

3.4. Examining the Base Shear in the Structure. The results from the base shear of the studied frames under near-field earthquakes and in damping and without damping conditions are provided in Figures 15–17. By comparing the values related to the near-field, one can see that the frames have more shear under the near-field earthquakes. Also, after adding the viscoelastic dampers to the frames, the base shear

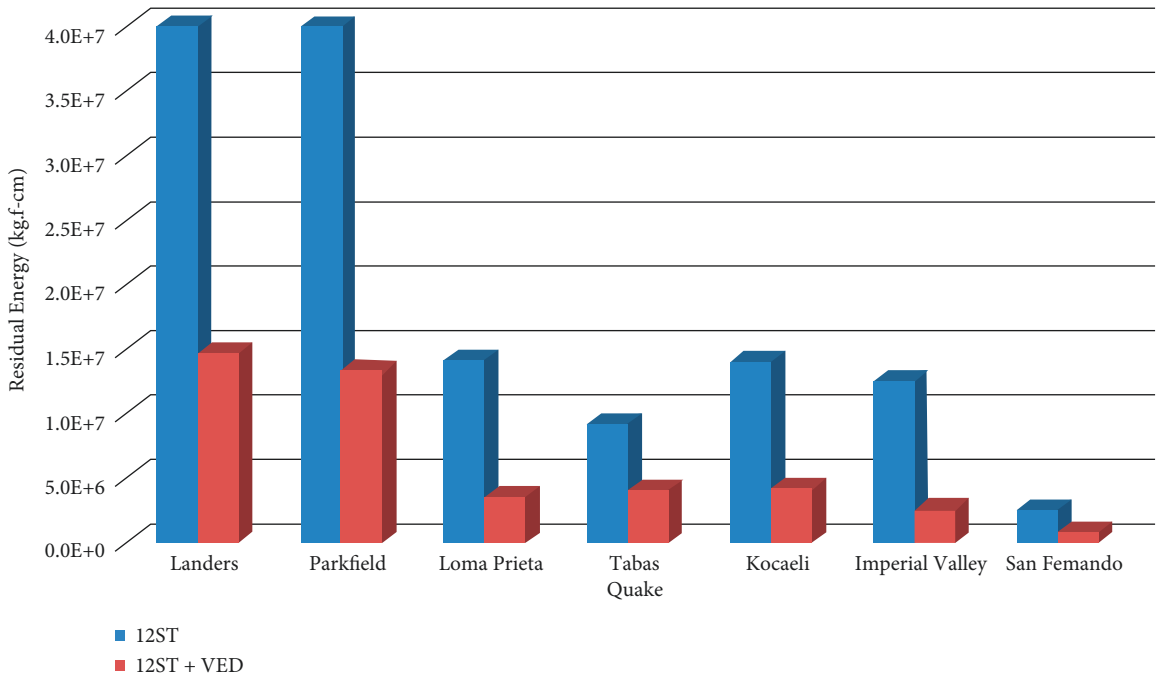

Figure 14: Residual energy diagram in a 12-story frame under near-field records, in two modes with and without dampers.

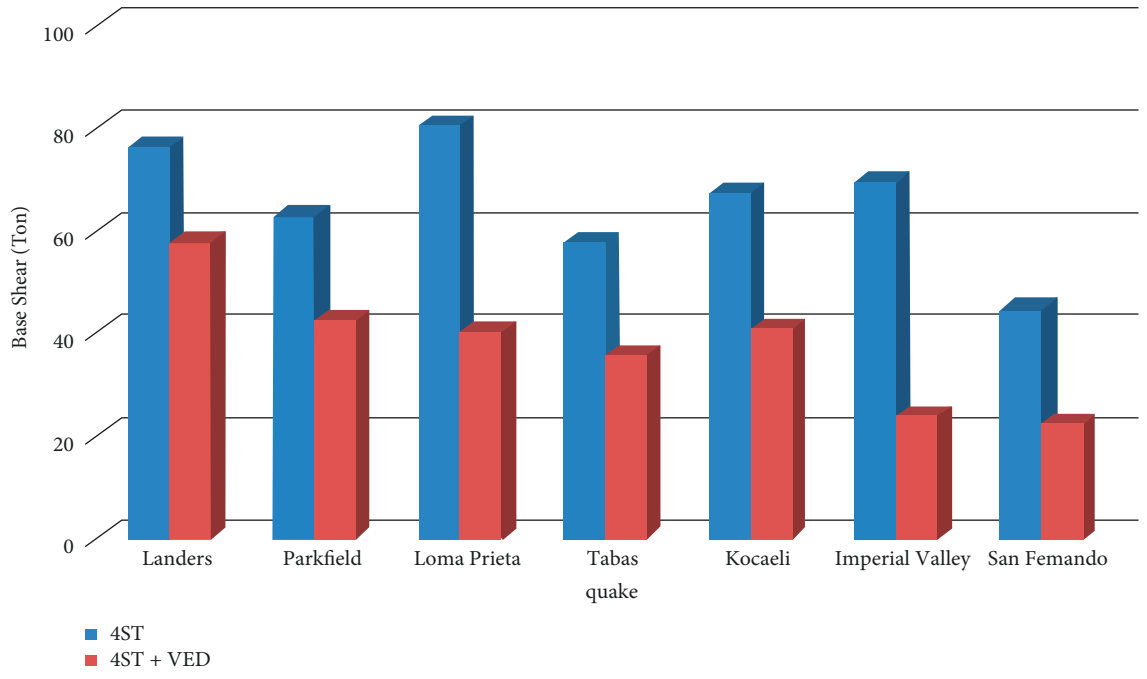

Figure 15: Shear base of a 4-story frame under near-field records in two modes with and without dampers (tons).

values are reduced. By controlling the allowable value according to the standard [47], all values were found to be within the allowable range of the regulations, and exceeding the allowable limits of the regulations which being equal to $V_{min} = 0.1$ AI Wt. is not less. Figure 15 show the results for the base section of a 4-story frame under near-field earthquakes for damped and damped conditions, respectively.

Figure 16 show the results for the base section of a 4-story frame under near-field earthquakes for damped and damped conditions, respectively.

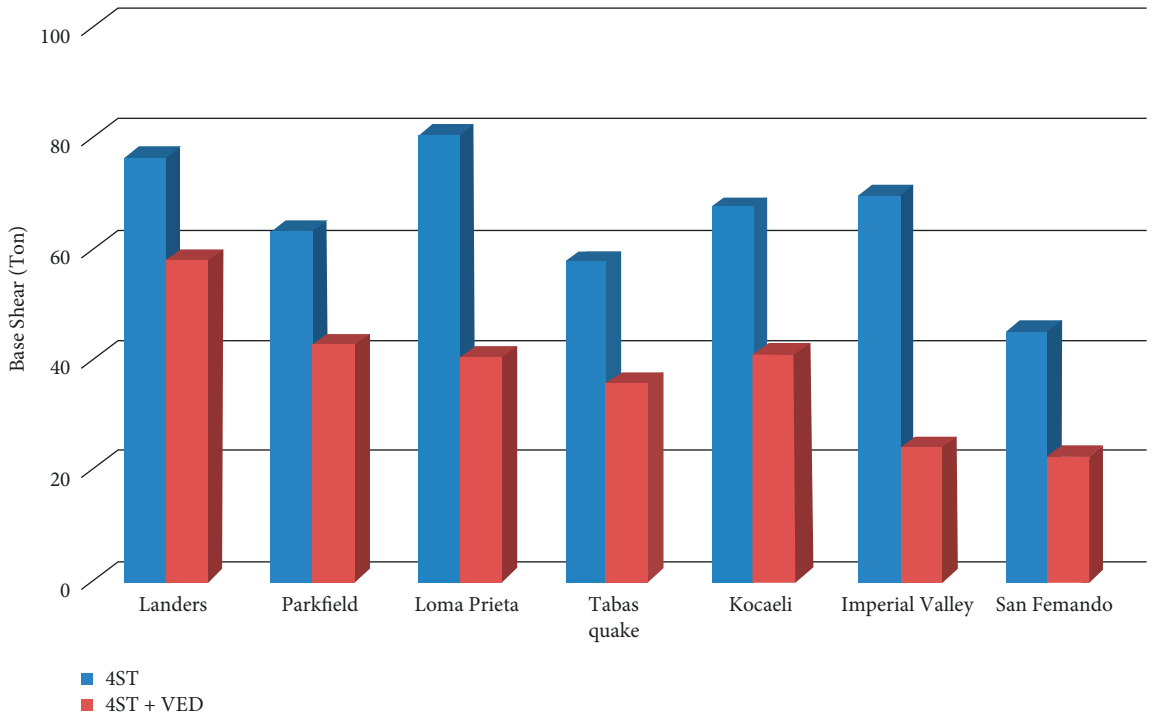

Figure 16: Shear base of an 8-story frame under near-field records in two modes with and without dampers (tons).

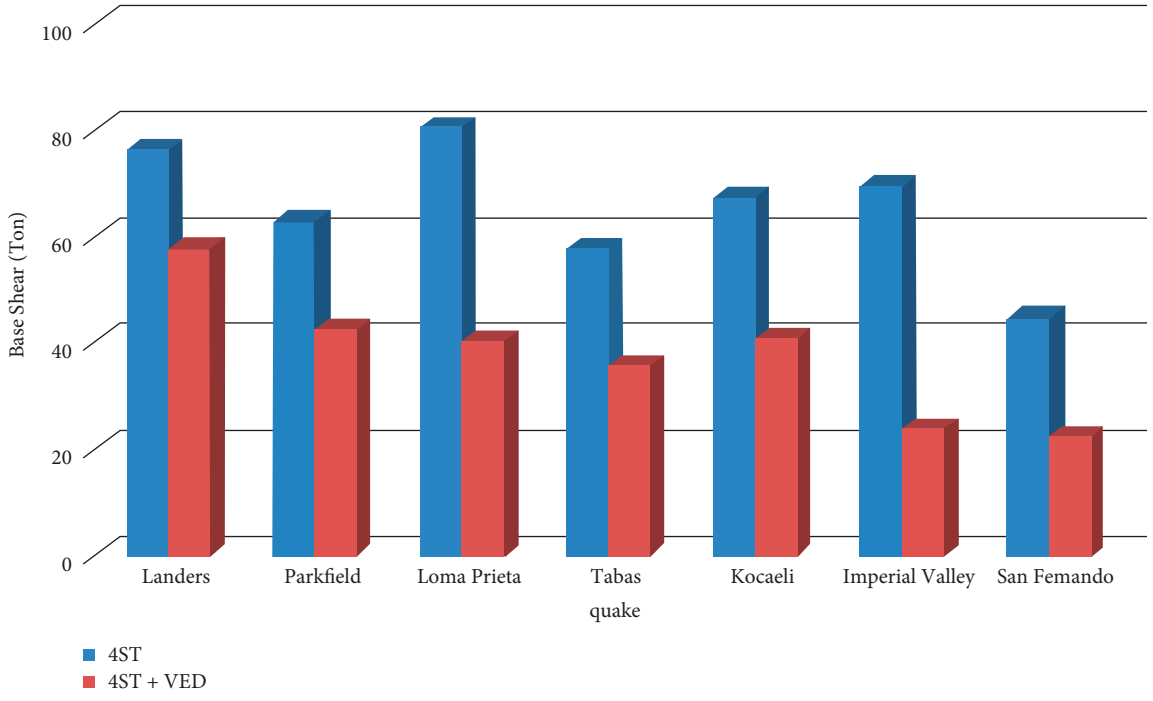

Figure 17: Shear base of a 12-story frame under near-field records in two modes with and without dampers (tons).

Figure 17 show the results for the base section of a 4-story frame under near-field earthquakes for damped and damped conditions, respectively.

3.5. Investigation of Roof Displacement in the Structure. The maximum displacement of the roof in centimeters under near-field earthquake with damping and without damping conditions is provided in Table 3. Also, as the height of the structure increases, the base shear values increase. As dampers are added to the structural layers, the base shear values are highly reduced. So that for 4, 8, and 12 floor frames under distant field earthquakes, 54%, 45%, and 48% decrease, respectively, and near-field earthquake decrease, 55%, 68%, and 64%, respectively.

Table 3: Roof displacement values in centimeters for near-field records.

Earthquake	4-story frame		8-story frame		12-story frame	
	No damper	Damper	No damper	No damper	Damper	No damper
Landers	32.4	18.0	48.6	67.2	302.8	55.8
Parkfield	25.2	12.0	76.8	58.6	136.8	61.2
Loma prieta	34.8	13.2	89.6	42.6	111.6	61.9
Tabas	18.0	8.6	39.7	30.4	122.4	36.0
Kocaeli	25.2	9.7	70.4	32.0	104.4	50.4
Imperial valley	14.4	6.5	60.5	18.6	33.5	18.4
San fernando	14.4	6.0	26.4	17.6	21.6	16.6

4. Conclusions

Damage to structures with the concept of inelastic behavior and, consequently, hysteresis energy is very close. Therefore, it can be said that hysteresis energy at these levels can be a significant criterion for designing or controlling the structure. The high dependence of hysteresis energy on structural damage has caused this concept and new structural design methods to be considered by researchers and engineers. Using viscoelastic dampers as a reinforcement method in the studied frames was found to have a great effect on reducing the relative floor displacement and reduced all values to the allowable range of the regulations, which is a also considered to be a reduction for earthquakes near the area after a damper is added. Viscoelastic dampers have been used for retrofitting. The results show that this type of damper has a great role in absorbing energy and reducing damage to buildings. Also, the effect of using viscoelastic dampers on reducing the damage of high-altitude frames has been more and shows good performance in reducing the damage under earthquakes in the near area. As the number of floors in the frames increases, the level of energy remaining in the structure increases because of earthquakes in the near and far areas. Using damper has great influence in residual energy to that extend in can reduce in till 75%. Because of the higher energy input, earthquakes in the area were very close. As dampers were added to the frames under study, the share of energy remaining in the structure and, consequently, the damage was significantly decreased. It is usually sought to reduce the damage by reducing the ratio of hysteresis energy to input energy in structures. In this study, it was seen that *ad* dampers were added to the frames, this ratio reduced to 90%, indicating the proper performance of viscoelastic dampers in reducing hysteresis energy absorption and damage. Roof displacement values are decreased between 30% and 75% using damper in 4-story to 12-story buildings. Also, shear base decrease 40% to 60% in these types of building only by considering these types of dampers in its structural elements. The results suggested that adding a damper to a greater frame produced better and reduced structural damage to a greater extent.

Data Availability

Requests for access to these data should be made to the author via e-mail address: javad.bashirpour@ut.ac.ir.

Conflicts of Interest

The author declares that there are no conflicts of interest regarding the publication of this paper.

References

[1] A. K. Chopra and E. F. Cruz, "Evaluation of building code formulas for earthquake forces," *Journal of Structural Engineering, ASCE*, vol. 115, no. 8, pp. 1881–1899, 1986.

[2] G. G. Hart, "Earthquake forces for the lateral force code," *The Structural Design of Tall Buildings*, vol. 9, pp. 49–64, 2000.

[3] Asce/Sei 7-16, *Minimum Design Loads for Buildings and Other Structures*, pp. 7–16, American Society of Civil Engineers, Virginia, USA, 2016.

[4] SEAO C. Vision, "A Framework for Performance Based Design," Technical report, Structural Engineers Association of California, Sacramento, CA, USA, 2000.

[5] A. K. Chopra, "Dynamics of structures: theory and applications to earthquake engineering," *Dynamics of Structures: Theory and Applications to Earthquake Engineering*, Prentice-Hall, New Jersey, NJ, USA, 2007.

[6] F. Y. Cheng, H. Jiang, and K. Lou, F. Y. Cheng, H. Jiang, and K. Lou, Smart structures: innovative systems for seismic response control," *Smart Structures: Innovative Systems for Seismic Response Control*, CRC Press, Boca Raton, Florida, 2008.

[7] S. Bungale, *Taranath "Wind and Earthquake Resistant Buildings Structural Analysis and Design"*, Marcel Dekker, New York, NY, USA, 2005.

[8] Z. Xu, X. Huang, F. Xu, and J. Yuan, "Parameters optimization of vibration isolation and mitigation system for precision platforms using nondominated sorting genetic algorithm," *Mechanical Systems and Signal Processing*, vol. 128, pp. 191–201, 2019.

[9] K. Chang, T T. Soong, S T. Oh, and M L. Lai, "Seismic Response of a 2/5 Scale Steel Structure with Added Viscoelastic Dampers," Technical Report NCEER-91-0012, University at Buffalo, New York, NY,USA, 1991.

[10] D. G. Lee, S. Hong, and J. Kim, "Efficient siesmic analysis of building structures with added viscoelastic dampers," *Engineering Structures*, vol. 24, no. 9, pp. 1217–1227, 2002.

[11] S. Tezkan and O. Uluca, *Reduction of Earthquake Response of Plane Frame Buildings by Viscoelastic Dampers*, Department of Civil Engineering, Boagzici University, Istanbul, Turkey, 2003.

[12] K. W. Min, J. Kim, and S. H. Lee, "Vibration tests of 5-storey steel frame with viscoelastic dampers," *Engineering Structures*, vol. 26, no. 6, pp. 831–839, 2004.

[13] M. Zimmer, "Characterization of Visco-Elastic Materials for Use in Seismic Energy Dissipation Systems," Master of Science Thesis, Department of Civil, Structural and Environmental Engineering, University at Buffalo, New York, NY, USA, 2000.

[14] M. S. E. Nasab and J. Kim, "Seismic retrofit of structures using hybrid steel slit–viscoelastic dampers," *Journal of Structural Engineering*, vol. 146, no. 11, Article ID 04020238, 2020.

[15] O. El-Khoury, A. Shafieezadeh, and E. Fereshtehnejad, "A risk-based life cycle cost strategy for optimal design and evaluation of control methods for nonlinear structures. Earthq Eng Struct Dyn:1–18El-Khoury O, Shafieezadeh A, Fereshtehnejad E (2018) A risk-based life cycle cost strategy for optimal design and evaluation of control methods for nonlinear structures," *Earthquake Engineering & Structural Dynamics*, vol. 1, p. 18, 2018.

[16] I. Gidaris and A. A. Taflanidis, "Performance assessment and optimization of fluid viscous dampers through life-cycle cost criteria and comparison to alternative design approaches," *Bulletin of Earthquake Engineering*, vol. 13, no. 4, pp. 1003–1028, 2015.

[17] N. M. Newmark and W. J. Hall, *Earthquake Spectra and Design"*, EERI, Berkeley, California, 1982.

[18] S. S. Golsefidi and S. A. Sahaf, "The effect of different loading patterns on the resistance to shear flow of hot mix asphalt," *Construction and Building Materials*, vol. 269, Article ID 121329, 2021.

[19] R. Lewandowski and Z. Pawlak, "Response spectrum method for building structures with viscoelastic dampers described by fractional derivatives," *Engineering Structures*, vol. 171, pp. 1017–1026, 2018.

[20] H. Shin and M. P. Singh, "Minimum life-cycle cost-based optimal design of yielding metallic devices for seismic loads," *Engineering Structures*, vol. 144, pp. 174–184, 2017.

[21] M. P. Singh, T. S. Chang, and H. Nandan, "Algorithms for seismic analysis of MDOF systems with fractional derivatives," *Engineering Structures*, vol. 33, pp. 2371–2381, 2011.

[22] H. Banon and D. Veneziano, "Seismic safety of reinforced concrete members and structures," *Earthquake Engineering & Structural Dynamics*, vol. 10, no. 2, pp. 179–193, 1982.

[23] H. Iemura, "Earthquake failure criteria of deteriorating hysteretic structures," in *Proceedings of the Seventh World Conference of Earthguake Engineering*, pp. 8–13, Istanbol, Istanbul, Turkey, July 1980.

[24] J. P. T. Yao and W. M. Unze, "Low cycle fatigue behaviour of mild steel," *ASTM Special Publication*, vol. 338, pp. 5–24, 1968.

[25] K. Wei, Q. Yang, Y. Dou, F. Wang, and P. Wang, "Experimental investigation into temperature-and frequency-dependent dynamic properties of high-speed rail pads," *Construction and Building Materials*, vol. 151, pp. 848–858, 2017.

[26] A. Chopra, *Dynamic of Structures Theory and Applications to Earthquake Engineering*, Prentice-Hall, New Jersey, NJ, USA, 2000.

[27] A. R. Ghaemmaghami and O.-S. Kwon, "Nonlinear modeling of MDOF structures equipped with viscoelastic dampers with strain, temperature and frequency-dependent properties," *Engineering Structures*, vol. 168, pp. 903–914, 2018.

[28] Weber, Feix, G. Feltrin, and O. Hath, "Guidelines for Structural Control," SAMCO Final Report, Structural Engineering Research Laboratory, Swiss Federal Laboratories for Materials Testing and Research Dübendorf, Switzerland, Europe, 2006.

[29] B. J. Kawak, B. H. Cabon, and G. S. Aglietti, "Innovative viscoelastic material selection strategy based on dma and mini-shaker tests for spacecraft applications," *Acta Astronautica*, vol. 131, pp. 18–27, 2017.

[30] A. M. G. De Lima, D. A. Rade, H. B. Lacerda, and C. A. Araújo, "An investigation of the self-heating phenomenon in viscoelastic materials subjected to cyclic loadings accounting for prestress," *Mechanical Systems and Signal Processing*, vol. 58-59, pp. 115–127, 2015.

[31] M. H. Mehrabi, M. Suhatril, Z. Ibrahim, S. S. Ghodsi, and H. Khatibi, "Modeling of a viscoelastic damper and its application in structural control," *PLoS One*, vol. 12, Article ID e0176480, 2017.

[32] S. M. Nigdeli and G. Bekdas, "Optimum tuned mass damper design for preventing brittle fracture of RC buildings," *Smart Structures and Systems*, vol. 12, no. 2, pp. 137–155, 2013.

[33] A. Li, "Viscoelastic damper," in *Vibration Control for Building Structures*Springer Tracts in Civil Engineering, Cham, Germany, 2020.

[34] P. Castaldo, *Integrated Seismic Design of Structure and Control Systems*, Springer, New York, NY, USA, 2016.

[35] E. Tubaldi, L. Ragni, and A. Dall'Asta, "Probabilistic seismic response assessment of linear systems equipped with nonlinear viscous dampers," *Earthquake Engineering & Structural Dynamics*, vol. 44, no. 1, pp. 101–120, 2015.

[36] D. Marriott, "A direct displacement-based seismic design procedure for moment frames with non-linear viscous dampers-part 2: validation of the design procedure," *SESOC Journal*, vol. 30, no. 2, p. 45, 2017.

[37] H. Jiang, S. Li, and Y. Zhu, "Seismic performance of high-rise buildings with energy-dissipation outriggers," *Journal of Constructional Steel Research*, vol. 134, pp. 80–91, 2017.

[38] Z. Lu, K. Li, and Y. Zhou, "Comparative studies on structures with a tuned mass damper and a particle damper," *Journal of Aerospace Engineering*, vol. 31, no. 6, Article ID 04018090, 2018.

[39] Q.-X. Shi, F. Wang, P. Wang, and K. Chen, "Experimental and numerical study of the seismic performance of an all-steel assembled Q195 low-yield buckling-restrained brace," *Engineering Structures*, vol. 176, pp. 481–499, 2018.

[40] B. Wang and S. Zhu, "Seismic behavior of self-centering reinforced concrete wall enabled by superelastic shape memory alloy bars," *Bulletin of Earthquake Engineering*, vol. 16, pp. 479–502, 2017.

[41] T. T. Soong and G. F. Dargush, *Passive Energy Dissipation Systems in Structural Engineering"*, Wiley, New York, NY, USA, 1997.

[42] A. Genovese, F. Carputo, A. Maiorano, F. Timpone, F. Farroni, and A. Sakhnevych, "Study on the generalized formulations with the aim to reproduce the viscoelastic dynamic behavior of polymers," *Applied Sciences*, vol. 10, no. 7, p. 2321, 2020.

[43] S. M. Seyed Kolbadi, H. Davoodian, and S. M. S.Kolbadi, "Evaluation of nonlinear behavior of reinforced concrete frames by explosive dynamic loading using finite element method," *Civil Engineering Journal*, vol. 3, no. 12, pp. 1198–1207, 2018.

[44] M. Barkhori, S. Maleki, M. Mirtaheri, M. Nazeryan, and S. M. S. Kolbadi, "Investigation of shear lag effect on tension members fillet-welded connections consisting of single and double channel sections," *Structural Engineering & Mechanics*, vol. 74, no. 3, pp. 445–455, 2020.

[45] G. Powell, "Nonlinear dynamic analysis capabilities and limitations," *The Structural Design of Tall and Special Buildings*, vol. 15, no. 5, pp. 547–552, 2006.
[46] K. C. Chang, S. J. Chen, and M. L. Lai, "Inelastic beheavior of steel frames with added viscoelastic dampers," *Journal of Structural Engineering*, vol. 122, 1996.
[47] M. A. Hariri-Ardebili and S. M. Seyed-Kolbadi, "surface method for material uncertainty quantification of infra-structures," *Shock and Vibration*, vol. 2018, Article ID 1784203, 15 pages, 2018.